

Wiener Filter for Short-Reach Fiber-Optic Links

Daniel Plabst, Javier García Gómez, Thomas Wiegart, *Student Member, IEEE*,
Norbert Hanik, *Senior Member, IEEE*

Abstract—Analytic expressions are derived for the Wiener filter (WF), also known as the linear minimum mean square error (LMMSE) estimator, for an intensity-modulation/direct-detection (IM/DD) short-haul fiber-optic communication system. The link is purely dispersive and the nonlinear square-law detector (SLD) operates at the thermal noise limit. The achievable rates of geometrically shaped PAM constellations are substantially increased by taking the SLD into account as compared to a WF that ignores the SLD.

Index Terms—Digital Dispersion Equalization, Wiener Filter, LMMSE Estimator, Intensity Modulation/Direct Detection (IM/DD), Geometric Shaping, Short-Haul Fiber-Optic Communication.

I. INTRODUCTION

SHORT-reach fiber-optic communications systems, e.g., for data-center interconnects, usually use transceivers based on intensity-modulation (IM) and direct detection (DD) (e.g., [1], [2]). Compared to coherent transceivers, IM/DD transceivers offer lower power consumption and hardware complexity, smaller form factors and hence reduced overall costs [1], [3]. To further reduce cost and complexity, short-link communication systems are usually operated without optical amplification and dispersion compensating fiber and require signal distortions to be compensated digitally at the receiver.

In short-reach communication systems, inter-symbol-interference (ISI) caused by chromatic dispersion (CD) is the limiting effect [2], [3], [4]. CD is described by a complex-valued impulse response. A DD receiver consists of a photodiode which measures the intensity of the imminent electrical field, and hence discards phase information. This complicates CD removal. Due to the absence of amplifiers on short-reach links, the square-law detector (SLD) is the only noise source. Since the receive signal is significantly attenuated, the SLD is assumed to operate at the thermal noise limit and adds white Gaussian noise to the intensity measurements [5, P. 154].

Common CD equalizers include linear feed-forward equalization (FFE) or non-linear methods like decision feedback equalizing (DFE), Volterra series based equalization, and neural network based equalization (e.g., [3, Sec. IV], [6]). In this paper, we consider a linear equalizer, namely the minimum mean square error (MMSE) estimator, also known as the Wiener filter (WF). We derive analytic expressions for the WF coefficients for short-reach IM/DD systems. Due to small

transmit signal powers, the Kerr nonlinearity of the link can be neglected [5, P. 65] and the link is purely dispersive.

In [7] the authors compute the WF assuming either real-valued Gaussian transmit symbols and a real-valued channel matrix or circularly symmetric complex Gaussian transmit symbols and a complex-valued channel matrix. We consider real-valued transmit symbols, originating from any symmetric probability density function (PDF), and a complex-valued channel matrix and extend the expressions from [7].

Notation: Bold letters indicate vectors and matrices, non-bold letters express scalars. For a matrix \mathbf{A} , we denote complex conjugate, transpose and Hermitian transpose by \mathbf{A}^* , \mathbf{A}^T and \mathbf{A}^H , respectively. The Hadamard product and the trace operator are expressed by \circ and $\text{tr}(\cdot)$, respectively. By $\text{diag}(\mathbf{a})$ we denote a square matrix with the vector \mathbf{a} on its main diagonal, while $\text{diag}(\mathbf{A})$ outputs the main diagonal of \mathbf{A} as a column vector. The $N \times N$ identity matrix is written as $\mathbf{I}_{N \times N}$, while the $N \times 1$ all-ones and all-zeros vector are referred to by $\mathbf{1}_N$, $\mathbf{0}_N$, respectively. The mean of a random vector \mathbf{a} is expressed by $\mu_{\mathbf{a}}$ and the covariance matrix of two random vectors \mathbf{a} , \mathbf{b} is denoted by $\mathbf{C}_{\mathbf{ab}}$. By \mathbf{e}_i , we denote the canonical unit (column) vector of appropriate dimensions, with all entries equal to zero, except the i -th (0-based indexing). Dirac's delta is expressed by $\delta(t)$ and we use $\langle a(t), a(t) \rangle = \int_{-\infty}^{\infty} |a(t)|^2 dt$ to indicate the energy of $a(t)$. The sinc function is defined as $\text{sinc}(\pi s) = \sin(\pi s)/(\pi s)$. The Nyquist ISI-free property of a pulse $g(t)$ with symbol period T_s reads $g(t)|_{t=kT_s} = g(0)\delta[k]$, $\forall k \in \mathbb{Z}$. A pulse $g(t)$ has the $\sqrt{\text{Nyquist}}$ property, if $g(t) * g^*(-t)$ has the Nyquist property. The Fourier pair $a(t) = \mathcal{F}^{-1}\{A(f)\}$ and $A(f) = \mathcal{F}\{a(t)\}$, is denoted by $a(t) \circ \bullet A(f)$. By $f(\mathcal{A})$ we denote that the function $f(\cdot)$ is applied element-wise to the set \mathcal{A} , i.e., $f(\mathcal{A}) = \{f(a) | a \in \mathcal{A}\}$. By $\Re\{\mathbf{A}\}$ and $\Im\{\mathbf{A}\}$ we denote element-wise real and imaginary part of the complex-valued matrix \mathbf{A} , respectively.

II. SYSTEM MODEL

A. Transmitter Front-End

In Fig. 1, the transmitter is fed with *positive* and *real-valued*, random, discrete-time data *symbols* s_ν , where ν is the discrete time index. We have $s_\nu \in \mathcal{S}$ and modulation alphabet \mathcal{S} .

1) *Digital-to-Analog Converter (DAC):* For *ideal* digital to analog conversion of the s_ν , the DAC performs pulse shaping with symbol time T_s . The continuous-time DAC output $a(t)$ reads

$$a(t) = s(t) * g_{\text{tx}}(t) = \sum_{\nu=-\infty}^{\infty} s_\nu g_{\text{tx}}(t - \nu T_s) \quad (1)$$

with real-valued pulse-shaping filter $g_{\text{tx}}(t)$ and

$$s(t) = \sum_{\nu=-\infty}^{\infty} s_\nu \delta(t - \nu T_s). \quad (2)$$

Date of current version June 22, 2022.

Daniel Plabst, Javier García Gómez, Thomas Wiegart and Norbert Hanik are with the Institute for Communications Engineering (LNT/LÄIT), Technical University of Munich, Munich, Germany (e-mail: d.plabst@tum.de, javier.garcia@tum.de, thomas.wiegart@tum.de, norbert.hanik@tum.de). Javier García Gómez's work was supported by the German Research Foundation under Grant KR 3517/8-2.

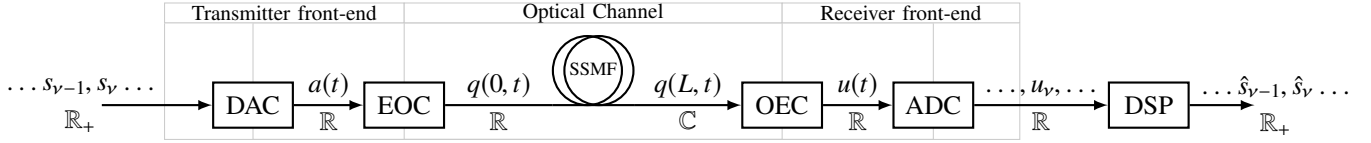


Fig. 1: Signal flow graph of a single-carrier IM/DD communication system.

2) *Electrical-Optical Converter (EOC)*: We use an *ideal* Mach-Zehnder Modulator (MZM) in push-pull mode [8, P. 19] as the EOC, which is shown in Fig. 2. The MZM modulates the amplitude of an electromagnetic carrier wave from a laser. The electric field $\bar{q}(t)$ of the laser light reads

$$\bar{q}(t) = E_0 \cdot e^{-j\omega_c t} \quad (3)$$

with $E_0 = \hat{E}_0 e^{j\phi_{E_0}(t)} \in \mathbb{C}$, $\hat{E}_0 \triangleq |E_0|$ and angular frequency ω_c . Laser fluctuations [5, P. 100] are neglected and we set $\phi_{E_0}(t) = 0$. Modulating $\bar{q}(t)$ with $x(t)$ leads to a complex-valued bandpass signal at the fiber input $z=0$ [8, P. 19]:

$$\bar{q}(0, t) = \underbrace{\cos\left\{x(t) \cdot \frac{\pi}{2V_\pi}\right\}}_{\text{Information signal } q(0, t)} \cdot \underbrace{\bar{q}(t)}_{\text{Carrier signal}} \quad (4)$$

with hardware constant V_π of the MZM and we set $V_\pi = \pi/2$. We decompose $x(t)$ into a bias $\bar{x} = \pi/2$ and alternating signal $\tilde{x}(t)$, i.e., $x(t) = \bar{x} + \tilde{x}(t)$, and use the small angle approximation for $\cos(\cdot)$ around \bar{x} , i.e., $\cos(\bar{x} + \tilde{x}(t)) \approx -\tilde{x}(t)$. The approximation error is small for $|\tilde{x}(t)| \ll \pi/2$. The bandpass signal $\bar{q}(0, t)$, launched into the fiber, reads as

$$\bar{q}(0, t) \approx -\hat{E}_0 \cdot \tilde{x}(t) \cdot e^{-j\omega_c t} \quad (5)$$

and we define $a(t) \triangleq -\hat{E}_0 \tilde{x}(t)$. Neglecting the carrier signal term from (5), we obtain the real-valued baseband signal

$$q(0, t) = a(t). \quad (6)$$

Modulating the *amplitude* of the baseband electric field modulates the optical *intensity* $I(z, t)$ at $z = 0$:

$$I(0, t) = \gamma_{\text{prop}} \cdot |q(0, t)|^2 = \gamma_{\text{prop}} \cdot a(t)^2 \quad (7)$$

with constant $\gamma_{\text{prop}} \triangleq 1$. For invertible relationships between amplitude and intensity, i.e., real-valued non-negative $a(t)$, this scheme is referred to as IM [8, P. 20]. Using a MZM, we require $a(t)$ to only be real-valued, but justify a non-negativity condition of the transmit symbols in Sec. IV-B.

B. Optical Channel

The propagation of the slowly varying signal $q \triangleq q(z, t)$ is described by the nonlinear Schrödinger equation [5, P. 65]

$$\frac{\partial q}{\partial z} = -j\frac{\beta_2}{2} \frac{\partial^2 q}{\partial t^2} + j\gamma|q|^2 q - \frac{\alpha}{2} q + n \quad (8)$$

where β_2 is the CD coefficient, γ is the Kerr nonlinearity parameter, α accounts for fiber-loss and z is the propagated distance. The term $n \triangleq n(z, t)$ describes noise realizations. The Kerr nonlinearity can be neglected for small optical transmit powers $P_{\text{tx, opt}}$ [5, P. 65]. With no amplification along the fiber, the dominant noise is added by the SLD at the receiver [1].

We thus set $n = 0$ and model electrical noise of the SLD in the following section. Finally, we consider attenuation in the signal-to-noise ratio (SNR) definition at the receiver and therefore simplify (8) to a *linear* differential equation

$$\frac{\partial q}{\partial z} = -j\frac{\beta_2}{2} \frac{\partial^2 q}{\partial t^2} \quad (9)$$

which can be solved analytically in the Fourier domain as

$$Q(L, \omega) = Q(0, \omega) \cdot e^{+j\frac{\beta_2}{2}\omega^2 L} \quad (10)$$

with $Q(\cdot, \omega) \bullet \circ q(\cdot, t)$, frequency response of CD $H(L, \omega) \triangleq e^{+j\frac{\beta_2}{2}\omega^2 L}$, $H(L, \omega) \bullet \circ h(L, t)$ and fiber length L .

C. Receiver Front-End

The receiver performs optical to electrical conversion (OEC), digitizes the signal by an ideal analog-to-digital converter (ADC) and recovers the transmitted data by DSP. The receiver in Fig. 3 consists of a *p-i-n* SLD [5, P. 153], with output current $r'(t)$ proportional to the intensity of the impinging electrical field, i.e., $r'(t) = \gamma_{\text{pd}} \cdot |q(L, t)|^2$, and proportionality constant $\gamma_{\text{pd}} \triangleq 1$ [5, Eq. (4.1.2-3)]. With no amplifiers on the fiber, $q(L, t)$ at the fiber end will be significantly attenuated compared to $q(0, t)$, which allows consideration of the receiver in the thermal noise limit [5, P. 154]. Therefore, $\eta'(t)$ is described by a *white* Gaussian random process with two-sided power spectral density (PSD) $\Phi_{\eta'\eta'}(f) = N_0/2$, autocorrelation function (ACF) $\phi_{\eta'\eta'}(\tau) = (N_0/2)\delta(\tau)$, time-lag τ and N_0 as stated in [5, Eq. 4.4.7]. With bandwidth limitation in the electrical filter $g_{\text{rx}}(t)$, prior to the ADC, the noise energy is finite and communication viable.

III. DISCRETE-TIME SYSTEM MODEL

A. Nyquist System

1) *Linear Case*: A *linear* communication system (Fig. 4 *without* SLD) with T_s -spaced sampling at the receiver has zero ISI, maximum SNR, and additive white Gaussian noise (AWGN) at the sampling times for $g(t) = g_{\text{tx}}(t) * h(L, t)$ being \sqrt{N} Nyquist and $g_{\text{rx}}(t)$ the matched filter [9, PP. 175].

2) *Nonlinear Case*: Consider the SLD, zero CD and a single symbol s_v being pulse-shaped and transmitted, which requires a \sqrt{N} Nyquist $r'(t)$ and $g_{\text{rx}}(t)$ as the matched filter. However, [10] showed that nonnegative, *bandlimited* \sqrt{N} Nyquist pulses do not exist and that practical nonnegative \sqrt{N} Nyquist pulses are time-limited to T_s . However, zero ISI and AWGN at the receiver at multiples of $T_s = 1/B$ are still viable, when, e.g., choosing $g_{\text{tx}}(t)$ as a *sinc* pulse shaping filter with bandwidth B , and $g_{\text{rx}}(t)$ as a *sinc* filter with bandwidth $2B$. Since *sinc* filters fulfill Nyquist and \sqrt{N} Nyquist criterion, the zero-ISI condition at T_s -spaced sampling is met and the receiver noise samples are uncorrelated, which we show in the following and Sec. IV-B.

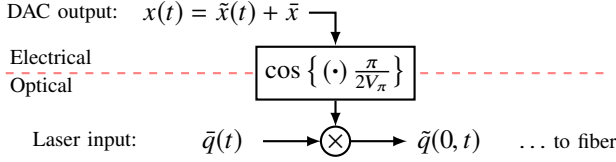


Fig. 2: A Mach-Zehnder Modulator as EOC.

3) *Nonlinear and Dispersive Case*: With CD, zero ISI at multiples of T_s is not viable, as a real-valued $g_{\text{tx}}(t)$ cannot form an ISI-free filter with the complex-valued CD $h(L, t)$. Thus, we formulate an optimization problem for the remaining ISI.

B. Bandlimited Sampling Receiver

We choose $g_{\text{tx}}(t) = \sqrt{B} \text{sinc}(B\pi t) \circ \bullet G_{\text{tx}}(\omega)$ as the unit energy, bandlimited transmitter pulse shaping filter, with two-sided bandwidth $B = 1/T_s$. With the number of transmit symbols V , the average *optical* transmit power $P_{\text{tx,opt}}$ per symbol reads

$$P_{\text{tx,opt}} \triangleq \lim_{V \rightarrow \infty} \frac{1}{VT_s} \mathbb{E}_s [\langle a(t), a(t) \rangle] = \frac{\sigma_s^2 + \mu_s^2}{T_s}. \quad (11)$$

We therefore adjust the average fiber launch power with the symbol variance σ_s^2 and mean μ_s . The receive filter $g_{\text{rx}}(t)$ has unit frequency gain and sets the receiver bandwidth to $2B$, i.e.,

$$g_{\text{rx}}(t) = 2B \cdot \text{sinc}(2B\pi t) \circ \bullet G_{\text{rx}}(f) = \begin{cases} 1, & \text{if } |f| \leq B \\ 0, & \text{otherwise} \end{cases} \quad (12)$$

given that the bandwidth from $q(L, t)$ to $r'(t)$ is doubled by the $|\cdot|^2$ -operation of the SLD. Thus, the receiver is a bandlimited sampling receiver, sampling $u(t)$ at $N_{\text{os}} \times B$, where $N_{\text{os}} \geq 2$ to avoid aliasing. The noise energy in $u(t)$ is thus finite. With real-valued transmit symbols, the PSD $\Phi_{\eta\eta}(f)$ and ACF $\phi_{\eta\eta}(\tau)$ of the bandlimited *real-valued* noise read [9, P. 233],

$$\Phi_{\eta\eta}(f) = \begin{cases} \frac{N_0}{2}, & \text{for } |f| \leq B \\ 0, & \text{otherwise} \end{cases} \bullet \circ \phi_{\eta\eta}(\tau) = \frac{N_0}{2} \phi_{g_{\text{rx}}g_{\text{rx}}}(\tau) \quad (13)$$

with $\phi_{\eta\eta}(\tau) = \phi_{\eta'\eta'}(\tau) * \phi_{g_{\text{rx}}g_{\text{rx}}}(\tau)$, $\phi_{g_{\text{rx}}g_{\text{rx}}}(\tau) = g_{\text{rx}}(\tau)$.

C. Discrete-Time Formulation

Sampling at $t = \nu T'_s$ with $T'_s = T_s/N_{\text{os}}$ and $N_{\text{os}} \geq 2$ gives

$$u(\kappa T'_s) \triangleq u[\kappa] = r'[\kappa] + \eta[\kappa] \quad (14)$$

where the discrete-time instant is $\kappa \in \mathbb{Z}$ and $\eta[\kappa]$ is zero-mean real-valued Gaussian noise with ACF $\phi_{\eta\eta}[\kappa] \triangleq \phi_{\eta\eta}(\tau = \nu T'_s)$. For $N_{\text{os}} = 2$, the noise is *white*, i.e., $\phi_{\eta\eta}[\kappa] = N_0 B \delta[\kappa]$ and therefore $\eta[\kappa] \sim \mathcal{N}(0, \sigma_\eta^2)$ with $\sigma_\eta^2 \triangleq N_0 B$ [9, P. 233]. Choosing $N_{\text{os}} > 2$ gives correlated noise and we thus set $N_{\text{os}} = 2$ for all remaining discussions. The noise-free $r'[\kappa]$ reads

$$r'_\kappa \triangleq r'[\kappa] = \left| \sum_{m=0}^{M-1} \psi[L, m] \cdot s'[\kappa - m] \right|^2 \quad (15)$$

where $s'_\kappa = s'[\kappa] \triangleq s(\kappa T'_s)$ by (2), i.e., the N_{os} -times upsampled version of the sequence $\{\dots, s_{\nu-1}, s_\nu, \dots\}$, and $\psi[L, \kappa] \triangleq \psi(L, \kappa T'_s)$ is the sampled, length M , combined impulse response (CIR) $\psi(L, t)$ of the transmitter pulse shaping filter and

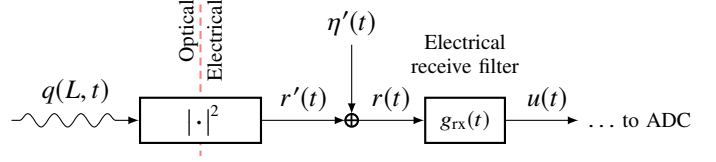


Fig. 3: Square-law detector as OEC with noise and receive filter.

CD, i.e., $\psi(L, t) \circ \bullet H(L, \omega) \cdot G_{\text{tx}}(\omega)$. Henceforth, we omit the argument L . Arranging $\mathbf{r}'[\kappa] = [r'_\kappa, \dots, r'_{\kappa+K-1}]^T$ gives

$$\mathbf{r}'[\kappa] = |\Psi' \cdot \mathbf{s}'[\kappa]|^2 \in \mathbb{R}_+^K \quad (16)$$

with standard linear convolution matrix $\Psi' \in \mathbb{C}^{K \times N}$, $N = K + M - 1$ with (right) shifted versions of the CIR vector $\psi = [\psi_{M-1}, \dots, \psi_0]^T$ arranged as its rows. The vector $\mathbf{s}'[\kappa] = [s'_{\kappa-M+1}, \dots, s'_\kappa, \dots, s'_{\kappa+K-1}]^T \in \mathbb{R}_+^N$ contains the upsampled transmit symbols. Note that by zero-insertion of upsampling,

$$s'_{\kappa+\Delta} = \begin{cases} s_\nu, & \text{if } (\kappa + \Delta) \text{ is even} \\ 0, & \text{otherwise} \end{cases} \quad (17)$$

with $\nu = \frac{\kappa+\Delta}{2}$ and $\Delta \in \mathbb{Z}$, following from $s'_\kappa \triangleq s(\kappa T'_s)$ by (2). We thus remove entries with odd index from the vector $\mathbf{s}'[\kappa]$ and denote the result as $\mathbf{s}[\kappa] \in \mathbb{R}_+^{N'}$. We also discard the according columns of Ψ' to get $\Psi \in \mathbb{R}^{K \times N'}$. Note that $|\cdot|^2$ is applied element-wise. The input-output relationship reads as

$$\mathbf{u}[\kappa] = \mathbf{r}'[\kappa] + \boldsymbol{\eta}[\kappa] = |\Psi \cdot \mathbf{s}[\kappa]|^2 + \boldsymbol{\eta}[\kappa] \in \mathbb{R}^K \quad (18)$$

and $\mathbf{u}[\kappa] = [u_\kappa, \dots, u_{\kappa+K-1}]^T$ and $\boldsymbol{\eta}[\kappa] = [\eta_\kappa, \dots, \eta_{\kappa+K-1}]^T$.

IV. WF PROBLEM STATEMENT

We now formulate the optimization problem to obtain the Wiener Filter [11, P. 382]:

$$\min_{\mathbf{g}, g_m} \text{MSE}, \quad \text{MSE} = \mathbb{E}_{\mathbf{s}, \boldsymbol{\eta}} \left| \hat{s}_\kappa - s'_\kappa \right|^2 \quad (19)$$

where the MSE is formulated between a single estimate $\hat{s}[\kappa] \triangleq \hat{s}_\kappa = \mathbf{g}^T \mathbf{u}[\kappa] + g_m$ with filter vector $\mathbf{g} \in \mathbb{R}^{K \times 1}$, filter mean $g_m \in \mathbb{R}$ and a single transmitted symbol s'_κ . Hence, s'_κ is linearly estimated from a vector of K measurements $\mathbf{u}[k]$. By (17), optimization (19) needs to *only* be solved for even κ .

A. WF Estimate

Letting κ be *even*, and omitting κ for vectors, the solution of (19) reads [11, P. 382],

$$\hat{s}_\kappa = \left(\mathbf{c}_{s'_\kappa}^T \mathbf{u} \mathbf{C}_{\mathbf{uu}}^{-1} \right) \cdot \mathbf{u} + \left(\mu_s - \mathbf{c}_{s'_\kappa}^T \mathbf{u} \mathbf{C}_{\mathbf{uu}}^{-1} \cdot \boldsymbol{\mu}_u \right) \triangleq \mathbf{g}^T \mathbf{u} + g_m \quad (20)$$

where the covariance matrices and mean vector compute as

$$\mathbf{c}_{s'_\kappa}^T \mathbf{u} = 2\sigma_s^2 \mu_s \cdot \Re \{ (\Psi \cdot \mathbf{e}_{M'}) \circ \mathbf{w}^* \}^T \quad (21)$$

$$\boldsymbol{\mu}_u = \sigma_s^2 \text{diag}(\Psi \Psi^H) + \mu_s^2 |\mathbf{w}|^{\circ 2} \quad (22)$$

$$\begin{aligned} \mathbf{C}_{\mathbf{uu}} &= \left(\mu_4 - 3\sigma_s^4 \right) \cdot |\Psi|^{\circ 2} \cdot |\Psi|^{\circ 2, T} \\ &+ \sigma_s^4 \cdot \left(\mathbf{z} \mathbf{z}^T + |\Psi \Psi^H|^{\circ 2} + |\Psi \Psi^T|^{\circ 2} \right) \\ &+ \sigma_s^2 \mu_s^2 \cdot \left[\mathbf{z} \cdot |\mathbf{w}|^{\circ 2, T} + |\mathbf{w}|^{\circ 2} \cdot \mathbf{z}^T \right. \\ &\left. + 2 \cdot \Re \{ \text{diag}(\mathbf{w}^*) \Psi \Psi^T \text{diag}(\mathbf{w}^*) \} \right] \end{aligned}$$

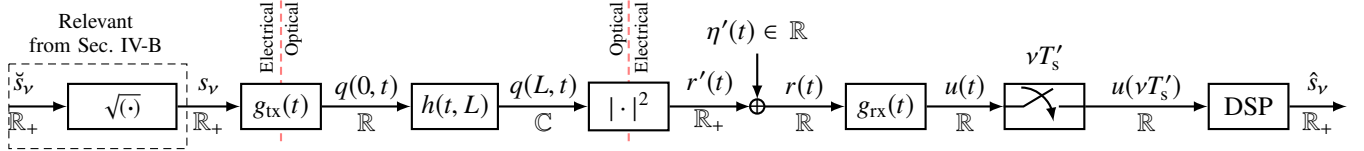


Fig. 4: End-to-end baseband model of the IM/DD lightwave communication system.

$$+ 2 \cdot \Re \left\{ \text{diag}(\mathbf{w}^*) \mathbf{\Psi} \mathbf{\Psi}^H \text{diag}(\mathbf{w}) \right\} \\ + \mu_s^4 \cdot |\mathbf{w}|^{\circ 2} \cdot |\mathbf{w}|^{\circ 2T} + \sigma_\eta^2 \cdot \mathbf{I}_{K \times K} - \boldsymbol{\mu}_u \boldsymbol{\mu}_u^T, \quad (23)$$

and $\mathbf{\Psi} \in \mathbb{C}^{K \times N'}$, $N' = M' + K' + 1$, with $M' = \lfloor \frac{M-1}{N_{\text{os}}} \rfloor$, $K' = \lfloor \frac{K-1}{N_{\text{os}}} \rfloor$ and vectors $\mathbf{w} = \mathbf{\Psi} \cdot \mathbf{1}_{N'}$, $\mathbf{z} = |\mathbf{\Psi}|^{\circ 2} \cdot \mathbf{1}_{N'}$. For computation of $\mathbf{C}_{\mathbf{u}\mathbf{u}}$ we assumed the transmit symbols s_v to be independently and identically distributed (iid) by a symmetric (around the mean) PDF with mean μ_s and variance σ_s^2 and denote the fourth-order *central* moment of s_v by μ_4 . All quantities (21)–(23) are real-valued, $\mathbf{C}_{\mathbf{u}\mathbf{u}}$ is positive definite and invertible. The noise is iid with $\eta[\kappa] \sim \mathcal{N}(\mathbf{0}_K, \mathbf{C}_{\eta\eta})$, where $\mathbf{C}_{\eta\eta} = \sigma_\eta^2 \cdot \mathbf{I}_{K \times K}$ and $\sigma_\eta^2 = N_0 B$. The WF can be pre-computed offline and efficiently applied using the FFT and overlap-add processing.

B. Mismatched WF

The s_v are iid by a symmetric probability mass function (PMF) with support \mathcal{S} . Considering Fig. 4 without CD, zero noise, $g_{\text{tx}}(0) \triangleq 1$ and Nyquist property of $g_{\text{tx}}(t)$ gives

$$u[\kappa] = \left(\sum_{\nu=-\infty}^{\infty} s_\nu g_{\text{tx}}(\kappa T_s' - \nu T_s) \right)^2 = \begin{cases} s_\nu^2 : \text{even } \kappa \\ \text{ISI} : \text{odd } \kappa \end{cases} \quad (24)$$

where for even κ , $\nu = \frac{\kappa}{2}$ by (17). The ISI corresponds to $u[\kappa]$ with odd κ and is discarded in this simple model. At even κ , we get the squared transmitted data. Choosing $s_v \in \mathbb{R}_+$ allows to unambiguously recover the transmitted symbols (already incorporated in Figs. 1,4). In addition, the receive symbols PMF has support $\mathcal{S}' = \{s^2 \mid s \in \mathcal{S}\}$, which makes it involved for a *linear* WF to map \mathcal{S}' onto \mathcal{S} . With AWGN, we also notice that symbols with smaller amplitudes are more affected by noise, which is undesired. From now on we include a pre-distortion block (cf. Fig. 4) in our discussions, which yields

$$s_v = \sqrt{\check{s}_v}, \quad \text{with } \check{s}_v \in \mathcal{S}, \quad s_v \in \sqrt{\mathcal{S}} \quad (25)$$

where \check{s}_v , s_v have mean $\check{\mu}_s$, μ_s and variance $\check{\sigma}_s^2$, σ_s^2 , respectively, leading to $s_v^2 \in \mathcal{S}$. Note that (25) is applied on the electrical side, i.e., in the transmitter DSP (cf. Fig. 4). Considering (25), the WF needs to be recomputed based on

$$\text{MSE}' = \mathbb{E}_{s, \eta} \left| \hat{s}_k - \sqrt{s_k'} \right|_2^2 \quad (26)$$

where in analogy to (17), for even κ and $\nu = \frac{\kappa}{2}$, we get $s_k' = \check{s}_v \in \mathcal{S}$ and $\sqrt{s_k'} = \sqrt{\check{s}_v} \in \sqrt{\mathcal{S}}$. To facilitate analytic expressions, we calculate a *mismatched* WF by approximating $\sqrt{\cdot}$ with a first-order Taylor series around the mean $\check{\mu}_s$ of \check{s}_v ,

$$\sqrt{\check{s}_v} \approx t_\alpha \cdot \check{s}_v + t_\beta \quad (27)$$

with constants $t_\alpha = 1/(2\sqrt{\check{\mu}_s})$, $t_\beta = \sqrt{\check{\mu}_s}/2$. We find the mismatched WF by substitutions for *all* quantities (21)–(23):

$$t_\alpha \check{\mu}_s + t_\beta \longrightarrow \mu_s; \quad t_\alpha^2 \check{\sigma}_s^2 \longrightarrow \sigma_s^2; \quad t_\alpha^4 \check{\mu}_4 \longrightarrow \mu_4 \quad (28)$$

where $\check{\mu}_4$ is the fourth-order central moment of \check{s}_v . We obtain the modified \mathbf{g}^T and g_m as a function of $\check{\mu}_s$, $\check{\sigma}_s^2$ and $\check{\mu}_4$,

$$\mathbf{g}^T = t_\alpha^{-1} \cdot \mathbf{c}_{s'_k \mathbf{u}} \mathbf{C}_{\mathbf{u}\mathbf{u}}^{-1}, \quad g_m = \check{\mu}_s - t_\alpha^{-1} \cdot \mathbf{c}_{s'_k \mathbf{u}} \mathbf{C}_{\mathbf{u}\mathbf{u}}^{-1} \cdot \boldsymbol{\mu}_u. \quad (29)$$

C. SNR Definition

Since noise is added on the electrical side, we define the SNR in the electrical domain [5, P. 153] and get the average electrical receive power as

$$P_{\text{rx,el}} = \frac{\sum_{\kappa=0}^{K-1} \mathbb{E}_s |r'(\kappa T_s')|^2}{N' N_{\text{os}}} = \frac{\text{tr}(\mathbf{C}_{\mathbf{r}'\mathbf{r}'}) + \|\boldsymbol{\mu}_{\mathbf{r}'}\|_2^2}{N' N_{\text{os}}} \quad (30)$$

with $\mathbf{C}_{\mathbf{r}'\mathbf{r}'}$ = $\mathbf{C}_{\mathbf{u}\mathbf{u}} - \mathbf{C}_{\eta\eta} \in \mathbb{R}^{K \times K}$, $\boldsymbol{\mu}_{\mathbf{r}'}$ = $\boldsymbol{\mu}_u \in \mathbb{R}^K$, where (21)–(23) are computed numerically using the *exact* moments of s_v . The electrical SNR after sampling is then given as

$$\text{SNR}_{\text{el}} = P_{\text{rx,el}} / \sigma_\eta^2. \quad (31)$$

For constant $P_{\text{tx,opt}} = \sigma_s^2 + \mu_s^2$, we remark that by (22)–(23), SNR_{el} depends on the particular choice of σ_s^2 , μ_s^2

D. Geometric Shaping

The achievable rate for different SNRs depends on the constellation mean μ_s and its variance σ_s^2 , with $\sigma_s^2 + \mu_s^2 = P_{\text{tx,opt}}$. In the following, we let $\check{s}_v \in \mathcal{S}$, where

$$\mathcal{S} = \left\{ P_{\text{tx,opt}} - \frac{D}{2} + \frac{i}{Q-1} D \right\}_{i=0}^{Q-1} \quad (32)$$

has equal-distance spaced elements and $D \leq 2P_{\text{tx,opt}}$ denotes the *constellation span*. Though not equivalent to rate, we use the *error to signal power ratio* (ESR),

$$\text{ESR} = \frac{\text{MSE}'}{\check{\sigma}_s^2} = 1 - \frac{\mathbf{c}_{s'_k \mathbf{u}} \cdot \mathbf{C}_{\mathbf{u}\mathbf{u}}^{-1} \cdot \mathbf{c}_{s'_k \mathbf{u}}^T}{\check{\sigma}_s^2} \quad (33)$$

as a proxy to find good values for σ_s^2 and μ_s for a particular SNR. Varying D for a fixed $P_{\text{tx,opt}}$, we obtain constellations $\sqrt{\mathcal{S}}$ with varying spacing and distance from zero, and thus varying μ_s and σ_s^2 . At low SNR, larger constellation spacing helps mitigate the effects of AWGN; at high SNR, constellations further away from zero lead to fewer SLD ambiguities.

V. NUMERICAL RESULTS

We consider a standard single-mode fiber (SSMF) at wavelength 1550 nm, with $\beta_2 = -2.168 \times 10^{-23} \text{ s}^2/\text{km}$, $\alpha = 0.046 \text{ km}^{-1}$, $\gamma = 1.27 \text{ W}^{-1} \text{ km}^{-1}$, link length $L = 20 \text{ km}$, receiver oversampling $N_{\text{os}} = 2$, symbol rate $B = f_{\text{sym}} = 27 \text{ GBaud}$ and modulation alphabets $\{4, 8, 16\}$ unipolar PAM. We transmit 100×10^3 symbols and set $P_{\text{tx,opt}} = \phi_{\text{max}} / (\gamma L_{\text{eff}})$, with maximal phase rotation $\phi_{\text{max}} = 0.1$, $L_{\text{eff}} = [1 - \exp(-\alpha L)] / \alpha$ [5, P. 64], where the Kerr nonlinearity becomes negligible and all

simulations are then carried out with $\gamma = 0$. The transmitter uses ESR-optimal geometric shaping and the receiver applies the WF. We choose the achievable rate from [12] as the performance metric, which is a lower bound on the mutual information of the channel. Comparisons are made to the capacity $\frac{1}{2} \cdot \log_2(1 + \text{SNR}_{\text{el}})$ of the real-valued AWGN channel, a CD-free back-to-back scenario ($L_{\text{btb}} = 0$ km) and a naive Wiener Filter $\overline{\text{WF}}$, which discards *all* non-linearities in Fig. 4. The naive $\overline{\text{WF}}$ computes in analogy to (20) with

$$\mathbf{C}_{\mathbf{u}\mathbf{u}} = \check{\sigma}_s^2 \Psi \Psi^H + \mathbf{C}_{\eta\eta}, \quad \mathbf{c}_{s',\mathbf{u}} = \check{\sigma}_s^2 (\Psi \mathbf{e}_{M'})^H, \quad \boldsymbol{\mu}_{\mathbf{u}} = \check{\mu}_s \Psi \cdot \mathbf{1}_{N'}$$

and we keep only the real part of its estimate. For both WFs, we set the number of considered observations to the length of the CIR, i.e., $K = M$. The sampled CIR $\psi(L, \kappa T'_s)$ is truncated and only elements larger than $\frac{1}{100} \cdot \max_{\kappa} \{|\psi(L, \kappa T'_s)|\}$ are kept in the vector ψ . We vary the electrical noise variance, σ_{η}^2 , in 5 dB steps from 0 dB to -110 dB. For comparison, we calculate the feasible SNR for a SLD [13] (marked in plots with vertical dashed line). This device has a single-sided noise-equivalent power $\text{NEP} = 21 \text{ pW}/\sqrt{\text{Hz}}$. With [5, P. 154], and single-sided bandwidth B of $g_{\text{rx}}(t)$, we get the feasible electrical SNR

$$\text{SNR}_{\text{feas,el}} = P_{\text{rx,el}} / (\text{NEP}^2 \cdot B) \quad (34)$$

where $P_{\text{rx,el}}$ is calculated according to (30) with the fiber attenuation considered in the channel matrix $\Psi^\dagger = \Psi \cdot e^{-\alpha/2 \cdot L}$. Fig. 5 (a) shows achievable rates for $L_{\text{btb}} = 0$ km and $L = 20$ km plotted against the SNR, when using geometric shaping with optimal normalized constellation span $D_{\text{norm}} = \frac{D}{2P_{\text{rx,opt}}}$ as given in Fig. 5 (b). For moderate fiber lengths L , the WF achieves the maximum mutual information with finite input alphabets asymptotically in SNR_{el} , as it is able to compensate CD and SLD-nonlinearity in the high-SNR regime. In addition, the WF significantly outperforms the suboptimal $\overline{\text{WF}}$, which saturates to the same rate for all used modulation formats. The achievable rate for the WF and $L_{\text{btb}} = 0$ km has a smaller slope compared to the AWGN channel, which is caused by the ISI of the pulse shaping filter (cf. (24)) and $N_{\text{os}} = 2$. Furthermore, for $L = 20$ km, the slope decreases further, as the derived WF is only Bayesian MSE optimal for jointly Gaussian observations \mathbf{u} and transmit symbols \check{y}_v , which is not fulfilled here [11, P. 379]. We also observe that the optimal constellation span in Fig. 5 (b) decreases in the SNR, as predicted in Sec. IV-D. For verification, Fig. 5 (c) shows the empirical ESR, where the MSE' (33) is calculated through simulations. Applying WF with geometric shaping results in a monotonically decreasing ESR, whereas the ESR for $\overline{\text{WF}}$ exhibits an error floor. The ESR can be used to predict the slope of the achievable rates for both fiber lengths. The WF with 8-PAM and SLD [13] allows transmission at 90 Gbit/s over 20 km with an ESR smaller than -20 dB. For reproducible results, all simulations are available on [14].

VI. CONCLUSION

We derived the WF for purely dispersive short-haul fiber-optical links with SLD. Together with a transmit constellation optimization, the WF compensates CD and SLD-nonlinearity and achieves the maximum rates for transmission over 20 km.

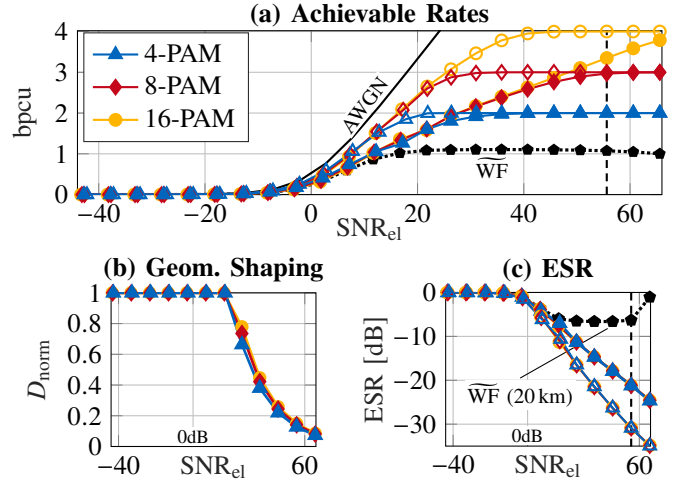


Fig. 5: (a) Achievable rates, (b) ESR-optimal constellation span, (c) ESR, versus SNR in dB. The vertical dashed line marks (34) using [13]. Empty and filled markers denote $L_{\text{btb}} = 0$ km (plots a, c) and $L = 20$ km (plots a, b, c), respectively.

For future work, imperfections in the transceiver can be addressed. In addition, the impact of the Kerr nonlinearity could be considered when transmitting at higher powers.

ACKNOWLEDGMENT

The authors wish to thank Prof. Gerhard Kramer and Prof. Amine Mezghani for useful suggestions and discussions.

REFERENCES

- [1] M. Chagnon, "Optical communications for short reach," *J. Lightw. Technol.*, vol. 37, no. 8, pp. 1779–1797, April 2019.
- [2] V. Houtsuma, D. van Veen, and E. Harstead, "Recent progress on standardization of next-generation 25, 50, and 100g epon," *J. Lightw. Technol.*, vol. 35, no. 6, pp. 1228–1234, 2017.
- [3] K. Zhong, X. Zhou, J. Huo, C. Yu, C. Lu, and A. P. T. Lau, "Digital signal processing for short-reach optical communications: A review of current technologies and future trends," *J. Lightw. Technol.*, vol. 36, no. 2, pp. 377–400, 2018.
- [4] S. Randel, D. Pileri, S. Chandrasekhar, G. Raybon, and P. Winzer, "100-gb/s discrete-multitone transmission over 80-km ssmf using single-sideband modulation with novel interference-cancellation scheme," in *2015 European Conference on Optical Communication (ECOC)*, 2015.
- [5] G. Agrawal, *Fiber-Optic Communication Systems: Fourth Edition*, 2010.
- [6] B. Karanov, M. Chagnon, F. Thouin, T. A. Eriksson, H. BÄijlow, D. Lavery, P. Bayvel, and L. Schmalen, "End-to-end deep learning of optical fiber communications," *J. Lightw. Technol.*, vol. 36, no. 20, pp. 4843–4855, 2018.
- [7] R. Ghods, A. S. Lan, T. Goldstein, and C. Studer, "Phaselin: Linear phase retrieval," in *2018 52nd Annual Conference on Information Sciences and Systems (CISS)*, 2018, pp. 1–6.
- [8] M. Seimetz, *High-order modulation for optical fiber transmission*. Springer, 2009, vol. 143.
- [9] R. Gallager, *Principles of Digital Communication*. Cambridge University Press, 2008.
- [10] S. Hranilovic, "Minimum-bandwidth optical intensity nyquist pulses," *IEEE Trans. Commun.*, vol. 55, no. 3, pp. 574–583, March 2007.
- [11] S. M. Kay, *Fundamentals of statistical signal processing*. Prentice Hall PTR, 1993.
- [12] F. J. Garcia-Gomez, "Numerically computing achievable rates of memoryless channels," *TUM University Library*, 2019. [Online]. Available: <https://mediatum.ub.tum.de/node?id=1533663>
- [13] Thorlabs Inc., "RXM40AF: 40GHz Amplified Photoreceiver," https://www.thorlabs.com/_sd.cfm?fileName=TTN179570-S01.pdf&partNumber=RXM40AF, 2019, [Online; accessed 20-March-2020].
- [14] D. Plabst, "Wiener Filter for Short Fiber-Optic Links," https://gitlab.lrz.de/dplabst/imdd_wiener_filter, 2020.